

Voltage-dependent scanning-tunneling microscopy of a crystal surface: Graphite

A. Selloni

Dipartimento di Fisica, Università La Sapienza, Roma, Italy

P. Carnevali

IBM Rome Scientific Center, Roma, Italy

E. Tosatti and C. D. Chen

International School for Advanced Studies, Trieste, Italy

(Received 23 July 1984; revised manuscript received 22 October 1984)

We discuss the possible application of the scanning-tunneling microscope (STM) to surface electronic spectroscopy, with an explicit calculation of the voltage-dependent tunneling current for an ideal STM experiment performed on graphite. We study how surface and bulk electronic states are reflected in the tunneling J - V spectra, and show that empty surface states of graphite may be well discriminated against bulk-like structures by considering STM spectra at different tip-surface separations.

The newly developed technique of scanning-tunneling microscopy has been proven to be very useful for the study of surface structures.¹ In usual applications the scanning-tunneling microscope (STM) is operated in the so-called constant-tunneling current mode: both the applied voltage V and the tunneling current J are kept fixed while the tip performs a lateral scan over the surface. The resulting surface of constant J , $z = z(x, y)$, is the STM "real space image" of the surface (z is the vertical position of the tip, while x and y are coordinates in the surface plane). Several theoretical papers have recently appeared, investigating the relationship between the STM images and the surface structure.²⁻⁴

In this Rapid Communication we discuss a different and so far unexploited application of STM, surface electronic spectroscopy. It is intuitively clear that vacuum tunneling into a surface should be stronger when the electron energy is such that it can flow into, or out from, a discrete surface state, or an important surface resonance (even if degenerate with bulk states). We show that the voltage dependence of the tunneling current may give important information on both filled and empty electronic states. In addition lateral scanning of the tip could be used to obtain a detailed picture of the spatial distribution of each energy-resolved electronic state.

We have chosen to illustrate our idea by direct calculation of the tunneling current J flowing into, or out of, a graphite surface, as a function of an applied voltage V . Our point is not to present a general theory of voltage-dependent tunneling, but rather to show—within a simplified tunneling model—how $J(V)$ is related to the surface electronic structure at energy $E - E_F = V$. Graphite has been chosen as an important test case, because both its atomic and electronic structures are well known. In particular, both localized σ and π states, as well as fairly delocalized interlayer states⁵ and recently discovered empty surface states,^{6,7} coexist within a range of a few eV around the Fermi energy. We suspect it might be technically difficult to achieve such large tunneling voltages over a semimetallic surface. Typical voltages yielding reasonably small currents such as 5×10^{-9} A are in the range of 10 mV in metal-metal tunneling.¹ However, it is not inconceivable that much higher voltages could be applied, for example, for very short times.

We calculate J using an approach similar to the one outlined in Ref. 2. Assuming an idealized tip with constant density of states D_t , we approximate the differential conductance dJ/dV as⁸

$$\frac{dJ}{dV} \propto \rho(\vec{r}, V) T(V). \quad (1)$$

Here, $\rho(\vec{r}, V)$ is the local density of states of the sample evaluated at the tip position² $\vec{r} = (x, y, z)$ and at energy $E = E_F + V$:

$$\rho(\vec{r}; V) = \sum_{n, \vec{k}} |\psi_{n, \vec{k}}(\vec{r})|^2 \delta(E_{n, \vec{k}} - E_F - V), \quad (2)$$

$\psi_{n, \vec{k}}(\vec{r})$ and $E_{n, \vec{k}}$ being the two-dimensional Bloch functions and the corresponding eigenvalues of the semi-infinite crystal in the absence of the tip. $T(V)$ is an approximate, \vec{k} -independent correcting factor which we introduce to account for the voltage drop in the vacuum region. We evaluate $T(V)$ assuming a triangular vacuum potential barrier and using the corresponding WKB expression for the transmission coefficient:

$$T(V) = \exp\left[-\frac{4}{3} \frac{\sqrt{2m}}{\hbar} \frac{z}{V} [\phi^{3/2} - (\phi - V)^{3/2}]\right] \times \exp\left[2 \frac{\sqrt{2m}}{\hbar} z (\phi - V)^{1/2}\right], \quad (3)$$

where ϕ is the work function (we assume both sample and tip to have the same value of ϕ). Implicit in this formula is the assumption that the decay of $\rho(\vec{r}, V)$ is purely exponential, with decay length $\hbar[2m(\phi - V)]^{-1/2}$. This assumption is reasonably well satisfied in our calculation, as shown in Fig. 2 below.

In order to calculate the local-state density (2), we replace the semi-infinite crystal with an n -layer slab of finite thickness $t = (n-1)c/2$, in a repeated slab geometry, where $c/2 = 3.35$ Å is the interlayer spacing in bulk graphite. The width of a vacuum region between adjacent slabs is $2c = 13.42$ Å. Four layers are sufficient for the purpose of describing most of the relevant features of $\rho(x, y, z; V)$, but slabs up to 10 layers thick are used, when needed, to investigate finer details.

The graphite slab electronic structure is obtained using a plane-wave representation, along with a carbon local pseudopotential⁹ empirically adjusted to give a reasonably accurate overall fit of *ab initio* linear-augmented plane-wave (LAPW) results for bulk graphite.⁵ Each slab is further encased within a square potential well along z . The well depth, $V_0 = 6.4$ eV, is chosen to yield a reasonable value, $\phi = 5$ eV, for the work function.¹⁰ The width d is empirically adjusted by the requirement that the interlayer and surface state should have approximately the same characteristics as in a self-consistent LAPW slab calculation.⁷ We find that $d = t + 0.75c$ is a satisfactory value. Calculating the energies of the empty surface and interlayer states at $\bar{k} = 0$ for slabs of increasing thickness, we find that, similarly to the results of Posternak, Baldereschi, Freeman, and Wimmer,⁷ two surface states split off below a band of bulklike states. For large thickness the split-off surface states lie about 0.1 eV below the $\bar{k} = 0$ bulk band bottom, a value compatible with the inverse photoemission data.⁶ The corresponding wave functions show a slow exponential decay into the vacuum. The decay length $\lambda = 0.63$ Å implies $E \sim -1/(4\lambda^2) \sim -2.4$ eV for the energy of the states relative to the vacuum, which well agrees with the calculated value.

Our plane-wave basis provides a good description of the delocalized interlayer states and empty surface states. On the other hand, many plane waves are required for a good description of the exponential decay of the wave function outside the surface. With a four-layer slab, we have used 705 plane waves (corresponding to a kinetic energy cutoff of 13 Ry) to obtain an exponential decay accurate over five orders of magnitude for the (x,y) averaged valence charge density. A somewhat poorer accuracy is usually obtained close to the "hollow" site because of the relatively low values of the corresponding charge density. Our total valence charge density for a four-layer slab is shown on Fig. 1, as a function of z , for (x,y) corresponding to "hollow" (S), "bridge" (SP), and "atop" (A) positions. The calculated corrugation at an average distance $z \sim 2$ Å from the

surface is 0.22–0.27 Å (the uncertainty being related to the above mentioned difficulties at the S site), which compares well with the He scattering values of 0.21–0.29 Å.¹¹

The use of empirical, not norm-conserving pseudopotentials to study wave-function properties might be generally questioned.¹² Of course, our reason for using a local pseudopotential is entirely one of convenience, and is only justified as a first approach. However, we stress that in the deep exponential decay region which is of interest for tunneling, the wave function, at given \bar{k} , is governed entirely by the state energy relative to vacuum, which is reasonably good in our calculation. For example, the energies (relative to vacuum) corresponding to (i) top of the filled σ band, (ii) π -bonding saddle point, (iii) π -antibonding saddle point, (iv) surface symmetric (antisymmetric) state, given by a monolayer LAPW as $-7.8, -6.9, -3.0, -1.2(-0.2)$ eV, respectively, are $-8.9, -7.6, -3.8, -2.8(-0.5)$ eV with our pseudopotential.

The (x,y) average $\bar{\rho}(z;V)$ of the four-layer slab local density of states $\rho(\bar{r};V)$ is plotted against z and for several values of V in Fig. 2. We have chosen values of V which select out successively different graphite states, i.e., top of the σ states at Γ ($V = -4$ eV), π states close to the Fermi energy ($V = 0$), empty π^* states at the M saddle point ($V = 1.3$ eV) and the empty surface state ($V = 2.5$ eV). A much slower decay is obtained for the latter. As a result, starting from a distance $z \sim 2$ Å from the surface, $\bar{\rho}$ at $V = 2.5$ eV is already about one order of magnitude larger than all relevant bulk structures. These features, and their consequences on the tunneling current $J(V)$, are made more evident in Fig. 3. Here, we show the voltage dependence of the tunneling conductance [Eq. (1)] for two different distances from the surface. We take $z = 2.5$ and 3.8 Å, which are presumably quite small as compared with typical tip-surface separations in present-day scanning-tunneling microscopy experiments (estimated values of z are in the range 4–10 Å¹⁻⁴). Although the main motivation for our choice of z is simply that our calculated charge density is not

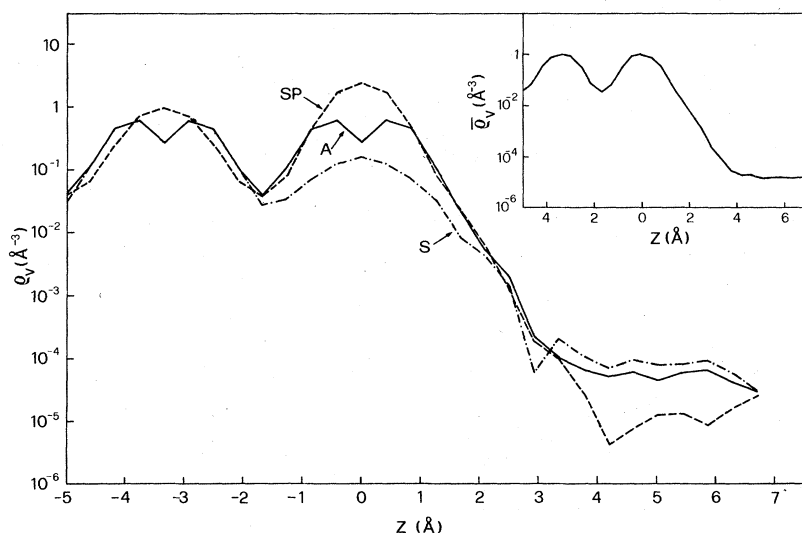


FIG. 1. Valence charge density $\rho_V(x,y,z)$ as a function of z for (x,y) corresponding to atop (full line), bridge (dashed line), and hollow (dotted line) sites on the surface plane. The inset shows the (x,y) averaged valence charge density. $z = 0$ coincides with a surface plane.

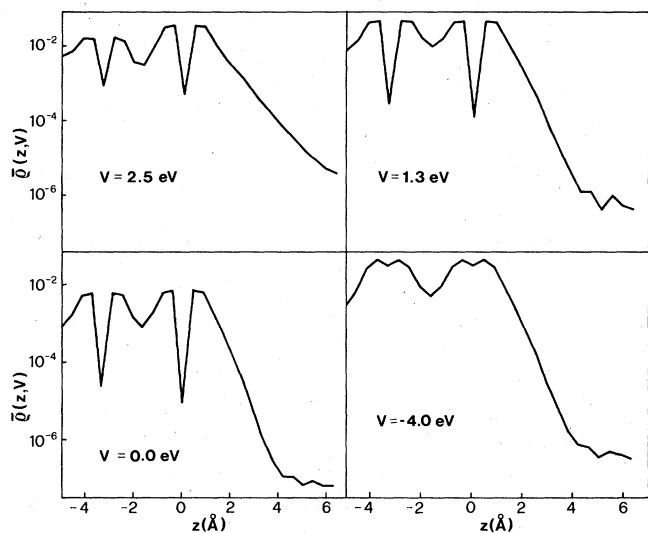


FIG. 2. z dependence of $\bar{\rho}(z, V)$ for σ states at $V \sim -4$ eV, π states close to the Fermi energy, π^* saddle point states at $V \sim 1.3$ eV, and surface states at $V \sim 2.5$ eV of a four-layer graphite slab. $z = 0$ coincides with a surface plane. $\bar{\rho}$ is in $\text{\AA}^{-3} \text{eV}^{-1}$ units.

well described beyond ~ 4 \AA , it is reasonable to believe that no significant new effect can occur between 4 and 10 \AA . Our results should thus remain very similar at larger distances. Bulk “resonant” features, such as saddle-point π and π^* states, as well as surface-state structures are clearly detectable in the tunneling conductance spectra of Fig. 3.¹³ It is also evident how, increasing the tip-surface separation, the relative importance of each structure changes, the surface-state peak becoming more important. We remark that this feature is contrasted but not offset by the exponential decrease of the “penetration factor” $T(V)$ [see Fig. 2 of Ref. 14, where $T(V)$ was omitted]. We also note that the surface to bulk state energy splitting (really of order 0.1–0.2 eV) is artificially increased in a four-layer slab. One should keep this in mind when extrapolating from the dJ/dV calculated curve of Fig. 3 to the real situation.

So far, we have shown only the (x, y) averaged tunneling conductance. Figure 4 illustrates the predicted voltage-dependent z corrugation for constant current of a graphite surface. We note that, while the corrugation is large near

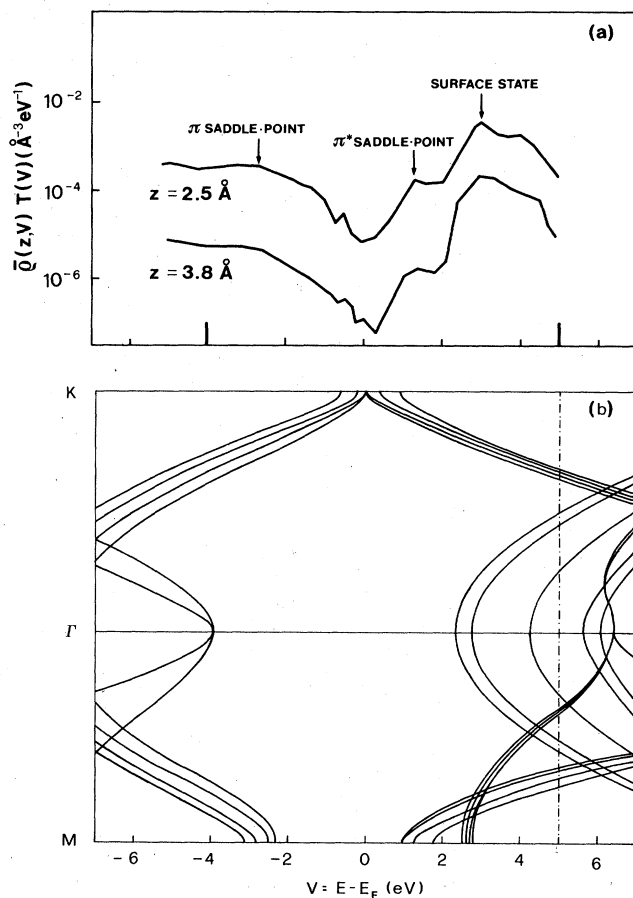


FIG. 3. (a) Voltage dependence of the (x, y) averaged tunneling conductance, given by Eq. (1), for different surface-tip separations. Tic marks at $V = -4$ eV and $V = +5$ eV refer to σ states and vacuum level. (b) Calculated band dispersions along ΓK and ΓM for a four-layer graphite slab.

the Fermi energy and for the π^* states, it is in fact very small for the surface state, which has a rather plane-wave nature in the (x, y) plane. The maximum height difference between S and A sites is approximately $\delta z = 0.7 - 1.0$ \AA around E_F ($V \sim 0$), $\delta z = 0.2 - 0.3$ \AA for π^* states ($V = 1.3$ eV), and $\delta z = 0.06$ \AA for the surface state. It is interesting

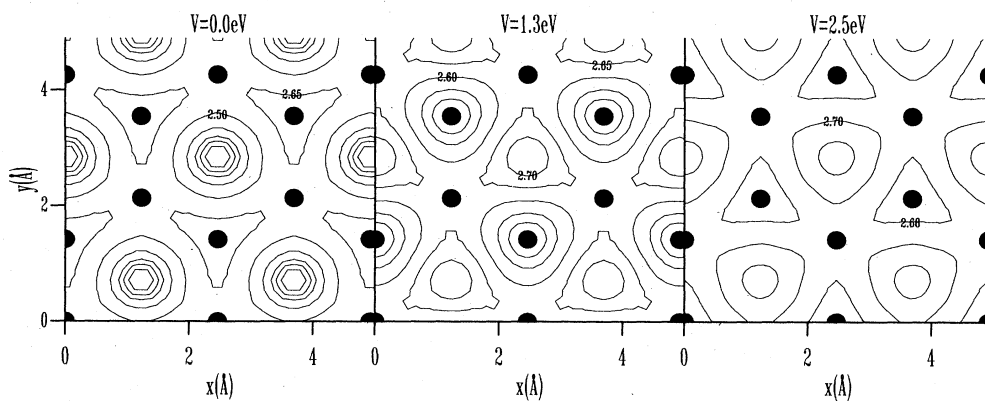


FIG. 4. Height-corrugation maps (in \AA) in the (x, y) plane for the various states shown on Fig. 2.

to remark how the corrugation amplitude at E_F is very much different from that of the total valence charge. This example points to the general fact that straight identification of STM maps with surface charge corrugation is not only in principle, but also in practice, clearly mistaken. A detailed study of the corrugation at the Fermi energy is in progress and will be reported elsewhere.

In conclusion, we have shown that voltage-scanned STM studies of surfaces, and in particular of a graphite surface,

should yield much important information on its electronic structure, very difficult so far to investigate with other means.

Note added in proof: The possibility of applying the STM to electronic surface-state spectroscopy was previously suggested by other authors. See, e.g., Refs. 15 and 16.

We acknowledge helpful comments by G. Binnig, D. R. Hamann, E. Stoll, and J. Tersoff.

¹G. Binnig, H. Rohrer, Ch. Gerber, and E. Weibel, *Phys. Rev. Lett.* **49**, 57 (1982); **50**, 120 (1983).

²J. Tersoff and D. R. Hamann, *Phys. Rev. Lett.* **50**, 1998 (1983).

³N. Garcia, C. Ocal, and F. Flores, *Phys. Rev. Lett.* **50**, 2002 (1983).

⁴E. Stoll, A. Baratoff, A. Selloni, and P. Carnevali, *J. Phys. C* **17**, 3073 (1984).

⁵M. Posternak, A. Baldereschi, A. J. Freeman, E. Wimmer, and M. Weinert, *Phys. Rev. Lett.* **50**, 761 (1983).

⁶Th. Fauster, F. J. Himpsel, J. E. Fischer, and E. W. Plummer, *Phys. Rev. Lett.* **51**, 430 (1983).

⁷M. Posternak, A. Baldereschi, A. J. Freeman, and E. Wimmer, *Phys. Rev. Lett.* **52**, 863 (1982).

⁸Restricting to *s*-wave tip wave functions (Ref. 2), the tunneling current at zero temperature is given by

$$J(V) \propto \int_{E_F}^{E_F+V} d\epsilon \tilde{\rho}(\bar{\Gamma}; \epsilon - E_F) D_t(\epsilon) ,$$

where $D_t(\epsilon)$ and $\tilde{\rho}(\bar{\Gamma}; \epsilon - E_F)$ are the tip density of states and the sample local density of states in the presence of an electric field of intensity V/z in the vacuum region. Equation (1) follows from this assuming $D_t = \text{const}$ and approximating $\tilde{\rho}(\bar{\Gamma}; \epsilon - E_F)$ by $\rho(\bar{\Gamma}; \epsilon - E_F)T(V)$. In the opposite limit of a delta-function-

shaped tip density of states, Eq. (1) would provide directly $J(V)$, rather than dJ/dV . Such simplifying assumptions for D_t are not meant to be realistic. In particular, $D_t = \text{const}$ may not be appropriate for a pointlike tip, i.e., a tip made up of a single atom or a small cluster of atoms.

⁹A. Baldereschi and C. D. Chen (private communication).

¹⁰The experimental value for the work function of graphite is 4.7 eV; see V. S. Fomenko, *Handbook of Thermionic Properties* (Plenum, New York, 1966).

¹¹W. E. Carlos and M. W. Cole, *Surf. Sci.* **91**, 339 (1980).

¹²D. R. Hamann, M. Schluter, and C. Chiang, *Phys. Rev. Lett.* **43**, 1494 (1979).

¹³The structure at $V = -0.5$ eV in Fig. 3 appears to be an artifact due to the relatively small number of \bar{k} points, $N_k = 150$, used for the calculation of $\rho(\bar{\Gamma}, E)$.

¹⁴A. Selloni, P. Carnevali, E. Tosatti, and C. D. Chen, *Proceedings of the 17th International Conference on the Physics of Semiconductors, San Francisco, 1984* (Springer-Verlag, New York, in press).

¹⁵A. Baratoff, in the *Proceedings of the Fourth General Conference of the European Physical Society, Condensed Matter Division* [Physica B (in press)].

¹⁶C. D. Chen, A. Selloni, and E. Tosatti, *Phys. Rev. B* (to be published).